Plant Physiology and Biochemistry 139 (2019) 707–714

Contents lists available at ScienceDirect

Plant Physiology and Biochemistry

journal homepage: www.elsevier.com/locate/plaphy

Research article

Soil management type differentially modulates the metabolomic profile of olive xylem sap

Adriano Sofo[a,*], Catia Fausto[a], Alba N. Mininni[a], Bartolomeo Dichio[a], Luigi Lucini[b]

[a] Department of European and Mediterranean Cultures: Architecture, Environment and Cultural Heritage (DiCEM), Università degli Studi della Basilicata, Matera, Italy
[b] Department for Sustainable Food Process, Università Cattolica del Sacro Cuore, via Emilia parmense 84, 29122, Piacenza, Italy

Keywords:
Olive tree
Plant chemical defense
Plant metabolomics
Soil sustainable management
Xylem sap

A B S T R A C T

In conventional olive growing, frequent soil tillage strongly reduces the complexity and diversity of the agro-ecosystem. Here, a metabolomic analysis was carried out on the xylem sap (XS) of olive plants (*Olea europaea* L.) from a grove located in Southern Italy (Basilicata region). The orchard has been divided in two plots that have been managed for 18 years with two different systems: a) 'sustainable management' (S_{mng}), with no-tillage, fertigation and internal C-inputs (spontaneous weeds and pruning residues), and b) an adjacent rainfed 'conventional management' (C_{mng}), that included soil tillage and mineral fertilization. The XS was extracted from olive shoots in two sampling times (ST1: May; ST2: October) using a Sholander pressure chamber, and its metabolome analyzed by ultra-high performance liquid chromatography (UHPLC) coupled to a hybrid quadrupole-time-of-flight mass spectrometer (QTOF-MS). The discriminating compounds were 94 at ST1 and 119 at ST2, and 35 of them were in common between the two sampling times. The majority of the discriminating metabolites (73 on 94 at ST1, and 109 on 119 at ST2) were found at higher concentration in the XS of S_{mng} plants, compared to that of C_{mng} ones. Most of the discriminating metabolites found in XS (about 80%, both at ST1 and ST2) were involved in plant secondary metabolism, mainly for plant chemical defense, growth regulation and signal transduction. The most prevailing class of compounds included terpenoids, phytohormones, alkaloids, sterols/steroids, retinols/retinoids, tocopherols and carotenoids. For the first time, we have demonstrated that the XS of a tree crop significantly responds to a shift of soil management. Generally, the plants of the S_{mng} plot showed an up-regulated secondary metabolism. The results of our study encourage the use of a set of sustainable agricultural practices in a productive orchard, in order to enhance plant physiological status, increase yield quantity/quality, safeguard the environment and ameliorate human health.

1. Introduction

Olive (*Olea europaea* L.) represents one of the most important oil crops world-wide, which has characterized the Mediterranean landscape since ancient times. In 2017, on an area of 10.65 Mha, 19.27 Mt of olives were harvested world-wide (FAOSTAT, 2017). Considering the relevance of this crop for semi-arid Mediterranean agricultural lands, a sustainable approach in olive orchard management is essential for improving soil quality, health and fertility (Sofo et al., 2014). The advantages of the adoption of a sustainable soil management that includes no/minimum tillage, cover crop application, incorporation of grass and pruning residues into the soil, and correct pruning, has been extensively studied in olive groves. Such benefits include a high level of soil microbial genetic/functional diversity and complexity both in the soil and in the phyllosphere (Sofo et al., 2014; Pascazio et al., 2015), a faster C and N turnover (Pascazio et al., 2018), higher levels of soil organic carbon (SOC) (Montanaro et al., 2012) and soil water content (Celano et al., 2011), and better soil physical (Palese et al., 2014) and chemical characteristics (Sofo et al., 2010).

The interactions between a plant and the composition of its xylem sap (XS) are highly complex and dynamic (Alvarez et al., 2008; Carella et al., 2016). The number and amounts of compounds in XS depend on some key factors, such as plant genotype and physiological status, sampled organ and tissue growth stage, sampling period, availability of soil nutrients, soil water potential and soil environmental conditions (Dambrine et al., 1995; Carella et al., 2016). If XS composition can be affected by differential agricultural practices is still a matter of debate, but no definitive findings are present in literature. Some attempts were

Abbreviations: PGP, Plant-growth promoting; ST, Sampling time; XS, Xylem sap

* Corresponding author.
E-mail addresses: adriano.sofo@unibas.it, adriano.sofo@libero.it (A. Sofo).

https://doi.org/10.1016/j.plaphy.2019.04.036
Received 1 December 2018; Received in revised form 26 April 2019; Accepted 26 April 2019
Available online 27 April 2019
0981-9428/

carried out with *in vitro* experiments. For instance, Lu et al. (2009) found that different nitrogen forms (NO_3^- or NH_4^+ applied in different proportions) affect cytokinin (CK) content in xylem sap of tomato seedlings, and that zeatin riboside is the main responsible for plant growth. Yong et al. (2000) applied elevated CO_2 (720 ppm) coupled with low mineral nutrition (2 mM NO_3^-) and observed a significant increase of CK content in cotton plants grown in greenhouse. Besides CKs, XP is also vehicle for other plant growth regulators such as indole-3-acetic acid and its derivatives (Sorce et al., 2002), and abscisic acid (ABA) (Alvarez et al., 2008).

Xylem sap is important for the transport of photosynthate and N-compounds throughout the plant body (Carella et al., 2016) and it contains a wide number of carbohydrates, amino acids, and proteins of different types and functions (Krishnan et al., 2011). Furthermore, plants can change XS composition when attacked by a microbial pathogen through the increase in the concentration of several phenylpropanoids, some amino acids and alkaloids, and other defense compounds (mainly phenolics, but also pentaketides and α-glucan, pullulan and stilbenes) (Bruno and Sparapano, 2006; Alvarez et al., 2008).

According to our knowledge, the information on how tree XS metabolome is modified by a different management system of an orchard is lacking. Very few studies (e.g., Ferguson et al., 1983; Sorce et al., 2002; Bruno and Sparapano, 2006; Lima et al., 2017) reported information on partial or complete sap metabolome in tree crops, and none of these dealt with the effects of agronomic practices on XS composition. Nonetheless, recent advances in metabolomics and related bioinformatics offer the possibility to gain a rather comprehensive picture on the phytochemical profile in biological systems, including plants, thus opening new opportunities (Meier et al., 2017; Tsugawa, 2018). On this basis, the main aim of this study was to investigate the xylem sap phytochemical profile of olive plants grown for 18 years under two different management systems, namely sustainable (S_{mng}) and conventional (C_{mng}). We hypothesized that a sustainable management system (S_{mng}) could cause significant differences in XS composition. A deepening about XS metabolome of olive plants grown under different agronomic systems could be useful for investigating the presence of compounds with plant-growth promoting (PGP) properties, that could be beneficial to the plants and promote the quality of this important fruit crop.

2. Materials and methods

2.1. Experimental site and olive grove management

The trial was carried out in a 2-ha mature olive grove (*Olea europaea* L., cv. 'Maiatica'; plants with an age of approximately 70 years, trained to vase at a distance of 8 × 8 m; NE orientation) located in Ferrandina (Southern Italy, Basilicata region; N 40°29′, E 16°28′) and managed using organic agricultural practices (sustainable management, S_{mng}) since 2000. The area has a semi-arid climate. In 2017, the annual precipitation was 645 mm (46 mm in ST1 and 68 mm in ST2, the two sampling dates), and the mean annual temperature ranged from 15 to 17 °C. The soil of the experimental grove is a sandy loam, classified as a Haplic Calcisol (FAO, 2006). The soil has a low gravel content and shows an increasing concentration of finely divided calcium carbonate particles in the soil matrix passing from the surface horizons (0.0–0.5 m) to the parental material (soil layer > 0.6 m). The major landform is plain, the slope form is classified as convex-straight and the slope gradient class as gently sloping (2–5%) (FAO, 2006). The depth of the groundwater at the moment of the analysis was > 1.5 m.

In the S_{mng} plot, olive plants were drip-irrigated from March to October (2800 $m^3\,ha^{-1}\,year^{-1}$) with six drip emitters discharging 8 $L\,h^{-1}$ over a 1-m radius around each plant. The top 60-cm soil layer had an average pH of 7.62 ± 0.36 (SD), total organic carbon content of 10.82 ± 0.58 $g\,kg^{-1}$, total N equal to 1.48 ± 0.28 $g\,kg^{-1}$, and C/N of 6.99 ± 1.19, with a mean bulk density of 1.37 $t\,m^{-3}$. The average annual amounts of organic C, N, P and K distributed by the irrigation water were 124, 54, 30 and 50 $kg\,ha^{-1}\,year^{-1}$, respectively. An integrative amount of 40 $kg\,ha^{-1}$ of $N{-}NO_3^-$ per year was distributed by fertirrigation during fruit set and pit hardening phase, in order to entirely satisfy the nutrient needs of olive trees. Plants were lightly pruned every year in winter. The soil was permanently covered by spontaneous self-seeding weeds (mainly Fabaceae and Poaceae), mowed twice a year for avoiding competition for water and nutrients. Cover crop residues and shredded prunings were shredded and left along the row as mulch.

An adjacent plot, characterized by soil and trees having similar features, was taken as control and conducted with a locally conventional management (C_{mng}), according to the practices usually adopted by farmers in the region. The top 60-cm soil layer had an average pH of 7.97 ± 0.31 (SD), organic carbon content of 9.78 ± 0.20 $g\,kg^{-1}$, total N equal to 1.05 ± 0.12 $g\,kg^{-1}$, and C/N of 9.32 ± 1.40, with a mean bulk density of 1.22 $t\,m^{-3}$. The C_{mng} plot was managed by tillage (milling at 10 cm depth) performed 2–3 times per year to control weeds. Severe pruning was carried out every two years, and pruned residues were removed from the olive orchard. Irrigation with aqueduct water was conducted empirically by the farmers, only if needed. A mineral fertilization was carried out once per year, in early spring, using ternary compounds (NPK 20-10-10 fertilizer at doses ranging from 300 to 500 $kg\,ha^{-1}\,year^{-1}$).

There were no diseases nor biotic stresses (e.g., drought, excess heat), nor N and P deficiency symptoms in the trees of both the management systems. There were no differences in tree height (about 4.0–4.5 m) and diameter between S_{mng} and C_{mng} plots, whereas yield in 2017 was 7.8 $t\,ha^{-1}$ in the S_{mng} plot and 4.3 $t\,ha^{-1}$ in the C_{mng} one.

2.2. Sap collection and extraction

The xylem sap (XS) was extracted from shoots of olive trees for both the management systems in May 2017 (sampling time 1: ST1) and in October 2017 (sampling time 2: ST2). In order to avoid border interferences, plants located in the central part of each plot and far 24 m each other were randomly chosen. For each treatment, three replicates (n = 3) of XS, each from one single plant, were collected using a Sholander pressure chamber (Model 600, PMS Instruments, Corvallis, OR) pressurized with N_2. This method was chosen because the application of pressure did not cause rapid sap changes with time and minimized the contamination of the extracted sap by cellular contents.

Two shoots, approximately 15–20 cm in length, were taken from each of the four cardinal points per plant using sterile cutting shears. The plant material was put in plastic bags, transported to the laboratory and stored 4 °C before use. For each shoot, a 1-cm wide bark strip was removed in the proximal part with a sharp knife sterilized with 75% ethanol, in order to exclude the phloem sap and to prevent external contamination. The cut end of the stem was placed in the pressure chamber facing out. The foliage of the cutting was placed in the pressure chamber and the lid was locked down. Then, high pressure was applied (approximately from 5.0 to 7.0 MPa, *i.e.* 50–70 bar) to force plant XS from the tissue at the proximal end of the cutting. After discarding the first drops, XS was collected into Eppendorf tubes for 15–20 min per shoot and centrifuged at 12,000 × g for 10 min at 4 °C. Thereafter, supernatants were taken and kept at −80 °C until metabolomic analysis.

2.3. Metabolomic analysis

Each individual XS sample was diluted in 10 vol of 1% HCOOH in 80% methanol, then filtered through a 0.22 μm disposable cellulose membrane into an amber vial for analysis. The untargeted screening of metabolites in XS was carried out through an ultra-high performance liquid chromatography (UHPLC) system coupled to a hybrid quadrupole-time-of-flight mass spectrometer (QTOF-MS) using previously the method described by Rouphael et al. (2016) with small modifications.

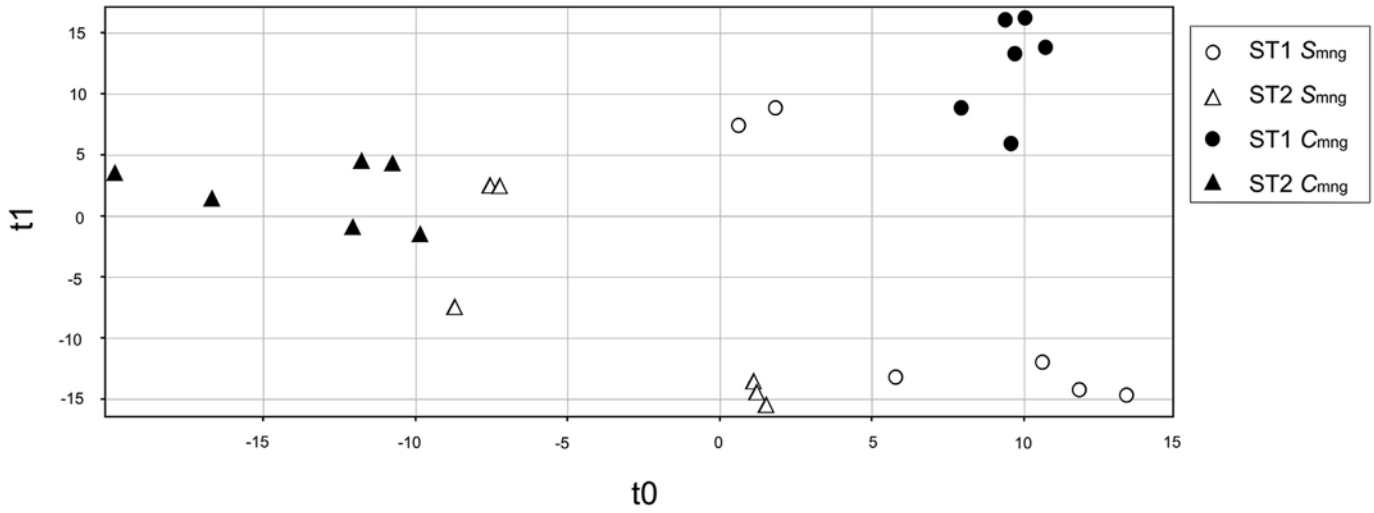

Fig. 1. Score plot from Partial Least Squares Discriminant Analysis (PLS-DA) multivariate analysis carried out from xylem sap metabolomic profile of olive plants grown either under sustainable (S_{mng}, white symbols) and conventional (C_{mng}, black symbols) soil management and at two different time points (ST1: May, circles; ST2: October, triangles).

The system included a 1290 liquid chromatograph, a G6550 iFunnel Q-TOF mass spectrometer and a Dual Electrospray JetStream ionization system (all from Agilent technologies, Santa Clara, CA, USA). Briefly, reverse phase chromatographic separation was achieved using an Agilent Zorbax Eclipse-plus C18 column (100 × 2.1 mm, 1.8 µm) and a mobile phase linear gradient (5%–95% methanol in water, 34 min run time) flowing at 220 µL min^{-1} at 35 °C. The mass spectrometer was run in positive ionization SCAN mode in the range of 100–1000 m/z^{+}. Each extract underwent a duplicate injection, and samples were randomly positioned in the analytical sequence; a blank (80% v/v aqueous methanol) was run after every three samples injection, whereas injection needle was washed for 8 s in 5% (v/v) HCOOH and 80% (v/v) acetonitrile following each injection.

Deconvolution and post-acquisition processing were done in Agilent Profinder B.06 using the 'find-by-formula' algorithm. After mass and retention time alignment, compounds annotation was achieved based on monoisotopic accurate mass (threshold < 5 ppm), isotopes spacing and isotopes ratio. With this aim, the database PlantCyc 12.5 (Plant Metabolic Network, http://www.plantcyc.org; released in April 2018) was used. Those compounds having an annotation score of > 75/100 were maintained in the dataset. Thereafter, a filter-by-frequency post-processing filter was applied to retain only those compounds that were present in 66% of replications within at least one treatment. Based on the strategy adopted, the identification was carried out according to Level 2 (putatively annotated compounds) of COSMOS Metabolomics Standards Initiative (http://cosmos-fp7.eu/msi).

The classification of the differential compounds into biochemical classes was carried following PubChem (NCBI, https://pubchem.ncbi.nlm.nih.gov/) and PlantCyc information.

2.4. Statistical analysis

The interpretation of metabolomic data ($n = 3$) was carried out using Mass Profiler Professional B.12.06, as previously described (Salehi et al., 2018). Briefly, compound abundance was Log_2 transformed and normalized at the 75th percentile and baselined against the median. Thereafter, a supervised multivariate analysis, Partial Least Square Discriminant Analysis (PLS-DA, N-fold validation) was also carried out. An accuracy threshold of 100% was adopted following N-fold validation. Variables loading plot, *i.e.* the weights used to build the PLS-DA class prediction model, were then displayed according to their importance within the latent vectors, and the most relevant ones (VIP - Variables of Importance in Projection) were exported from the covariance structures in the PLS-DA hyperspace.

Finally, analysis of variance (unpaired *t*-test, $p < 0.01$, Bonferroni multiple testing correction) and fold-change analysis (fold-change cut-off = 5) were combined into Volcano Plot pairwise comparisons. Venn analysis on Volcano-filtered compounds allowed identifying the differential compounds shared between the two time points from those exclusive of a single time point.

3. Results and discussion

3.1. Xylem sap extraction and discriminating metabolites

Because of the difficulty and laborious sap extraction technique, and to the high-tension gradient and very low leaf water potentials (up to −7.5 MPa in leaves) of olive plants (Dichio et al., 2006), limited amounts of XS were extracted from each shoot and the procedure was time-consuming. Thus notwithstanding, the method here used allowed to extract enough amounts of XS for the following metabolomic analysis.

For a long time, XS has been considered as containing only water and minerals, but various studies have successively demonstrated that it also contains metabolites and proteins (Mazzafera and Gonçalves, 1998; Sorce et al., 2002; Alvarez et al., 2008; Lu et al., 2009; Krishnan et al., 2011; Carella et al., 2016). In fact, more than 800 compounds were found in the XS of plants from either S_{mng} and C_{mng} plots. The whole list of compounds revealed in XS is provided as supplementary material, together with their abundances and composite spectra (mass and abundance combinations) (Supplementary Table S1).

Starting from this wide phytochemical profile, PLS-DA modelling allowed to classify samples into four groups, thus confirming a seasonal variability in XS composition and indicating that soil management has distinctively shaped XS metabolome (Fig. 1). Indeed, accuracy was 100%, with no misclassification following training and validation of the PLS-DA class prediction model. On this basis, the combination of ANOVA and fold-change analysis from Volcano Plot was used to identify differential metabolites, *i.e.* those differentiating the two management systems. Differential compounds were 94 for ST1 and 119 for ST2. Among these compounds, 35 were in common between the two sampling times, while 59 were found only at ST1 and 84 only at ST2 (Fig. 2). Most of the common metabolites were terpenoids with different numbers of carbon (C) atoms (mono-, di- and triterpenoids; 12 on 35), fatty acid compounds with a different degree of saturation (5), alkaloids (3), indole derivatives (3) and retinols (2). At ST1, 73 of the

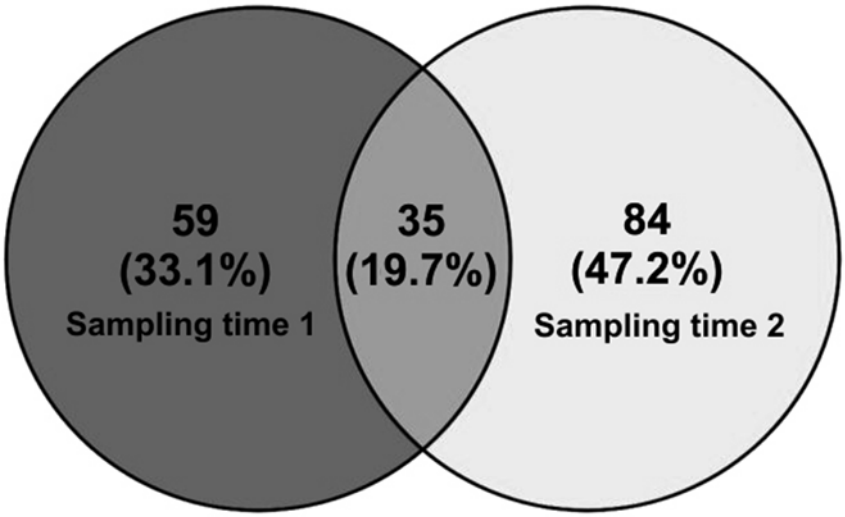

Fig. 2. Venn analysis from differential metabolites (as provided by Volcano Plot analysis, at $p < 0.01$ and fold-change > 5) in xylem sap, discriminating olive plants grown either under sustainable (S_{mng}) and conventional (C_{mng}) soil management at two different time points (ST1: May; ST2: October).

94 discriminating metabolites were found at higher concentration in the XS of S_{mng} plants and only 21 higher in that of C_{mng} plants (Table 1). At ST2, 109 of the 119 discriminating metabolites were found at higher concentration in plants from the S_{mng} plot and only 10 higher in those from the C_{mng} plot (Table 2).

3.2. Main classes of discriminating metabolites

Despite the discriminating metabolites belonged to heterogenous biochemical classes, a clear trend was observed. Indeed, only few compounds were primary metabolites, including some amino acids and amino acid-derivatives (8 detected at ST1 and 6 at ST2), as well as glycerol and fatty acid-derived compounds (16 at ST1 and 18 at ST2). Generally, the primary metabolism was only partially affected by the soil management adopted, as amino acids derivatives were generally over-represented in the XS of S_{mng} plants (Tables 1 and 2). Pascazio et al. (2018) have recently found that the irrigation method and soil management can deeply affect nitrogen (N) cycling in a sustainable olive grove, highlighting the contribution of soil bacteria in N transformations. In the XS, these change in N dynamics are likely reflected by different NO_2^-/NH_4^+ and asparagine contents (Mazzafera and Gonçalves, 1998), while other secondary metabolites, such as cytokinins and their purine-based precursors (Yong et al., 2000; Lu et al., 2009), alkaloids (Mazzafera and Gonçalves, 1998), and amino acids deriving from polypeptide hormones (Krishnan et al., 2011), can be more intensively regulated by different growth environments.

Regarding fatty acids derivatives, they were generally over-represented in the XS of S_{mng} plants, even if some cases of down-accumulation were observed (6 in ST1 and 2 in ST2). Interestingly, diacylglycerols at both ST1 and ST2 were down-represented in the XS of S_{mng} plants (Tables 1 and 2). This could reflect a change in hormonal balance, as these substances are not only membrane constituents and storage lipids, but also signaling lipids and precursor of phosphatidic acid (PA), with a pivotal role in the plant's response to environmental signals, through the PLC (phospholipase C)-DGK (diacylglycerol kinase) pathway (Arisz et al., 2009). This is supported by the fact that phosphatidyl compounds deriving from PA (1-16:0-2-lysophosphatidylcholine and 1-oleyl-2-lyso-phosphatidate at ST1, and 1-18:0-2-18:3-phosphatidylethanolamine at ST2) were higher in the XS of S_{mng} plants than in that of C_{mng} ones (Table 1).

Most of the discriminating metabolites (about 80%, both at ST1 and ST2) were involved in the secondary metabolism. Among them, the most prevailing class included terpenoids having different number of C atoms (25 at ST1 and 43 at ST2), phytohormones/plant growth regulators and their conjugates and derivatives (8 gibberellins, 5 auxins, 2 jasmonates, 2 cytokinins and 1 strigolactone at ST1; 4 auxins, 3 jasmonates, 1 gibberellin and 1 strigolactone at ST2); alkaloids (6 at ST1 and 12 at ST2); sterols/steroids (13 at ST1 and 2 at ST2); and retinols/retinoids, tocopherols and carotenoids (2 at ST1 and 6 at ST2) (Tables 1 and 2).

Plant terpenoids (or isoprenoids) are a large and diverse class of hydrocarbons composed of isoprene units. Unlike terpenes, from which they derive, they contain additional functional groups, usually with oxygen atoms, and most have multicyclic structures. Many plant terpenoids are repellant, due to their taste and smell, and/or toxic for a wide range of insects and fungi, so acting as a defense against herbivores, pathogens and parasites (Heldt et al., 2005; Singh and Sharma, 2015). The terpenoids with a direct effect on fungi are also included among 'phytoalexins' (Singh and Sharma, 2015) and were found to be more abundant in the XS of S_{mng} plants (kauralexin A2 at ST1; oryzalexin A, B, D, E, F, and kauralexin A1 at ST2) (Tables 1 and 2). Important monoterpenoid derivatives (10 C atoms) involved in plant defense against insects, such as a limonene-1,2-diol and (6*E*)-8-hydroxygeraniol, and (6*E*)-8-oxogeranial and a 7-hydroxy-4-isopropenyl-7-methyloxepan-2-one were found more abundant in the XS of S_{mng} plants (Tables 1 and 2). Other discriminating terpenoids are involved in phytohormone pathways (e.g., *trans*-abscisic alcohol for abscisic acid, 13-desoxypaxilline for indole-based auxins at ST2), carotenoids biosynthesis (prephytoene diphosphate at ST1), and sesqui- (15 C), di- (20 C) and triterpenoid (30 C) biosynthetic patterns. Most of them showed higher concentrations in plants subjected to a S_{mng} (Tables 1 and 2).

Many other plant secondary metabolites are biologically produced from terpenoid precursors, such as carotenoids and gibberellins (both have geranylgeranyl pyrophosphate as a precursor), steroids (from farnesyl pyrophosphate), cytokinins and quinones (Singh and Sharma, 2015; Lacombe and Achard, 2016). It is well known the antioxidant and protective action of carotenoids and their related (retinoids and retinols), even if their trend was not particularly clear, as they were up-accumulated in the XS of S_{mng} plants at ST2 but not at ST1 (Tables 1 and 2). Saponins, a class of glycosylated steroids, act as strong toxins against herbivores and fungi (Heldt et al., 2005). Oleanolate 3-β-D-glucuronoside-28-glucoside, medicagenate and 16-α-hydroxygypsogenate differentiated S_{mng} (higher levels) from C_{mng} plants at ST1 (Table 1), and all of them are precursors of saponins. Plant sterols are an essential component of cell membranes but, most interestingly, many of them act as

Table 1
Differential metabolites as provided by Volcano Plot analysis (*t*-test at $p < 0.01$ with Bonferroni multiple testing correction and fold-change > 5) in xylem sap metabolomic profile of olive plants grown under sustainable (S_{mng}) *vs* conventional (C_{mng}) soil at time point ST1 (May). Compounds are grouped in biochemical classes. The regulation (up or down) refers to the S_{mng} compared to C_{mng}.

Class	Compound	Regulation
Sterol lipids	poriferst-5,7-dienol	up
	avenasterol	up
	24-methylenelophenol	up
	4-alpha-14-alpha-dimethyl-9-beta-19-cyclo-5-alpha-cholest-24-en-3-beta-ol	up
	4-alpha-methyl-5-alpha-ergosta-8,24-dien-3-beta-ol	up
	poriferst-8,25(27)-dienol / poriferst-7,25(27)-dienol	up
	4-alpha-14-alpha-dimethyl-5-alpha-cholesta-8,24-dien-3-beta-ol	up
	17-alpha;-hydroxyprogesterone	up
	4,4-dimethyl-5-alpha-cholesta-8,14-dien-3-beta-ol	up
	4,4-dimethylzymosterol	up
	11-deoxycorticosterone	up
	isofucosterol	up
	Delta24-25 sitosterol	up
Other lipids	decanoate	up
	1-oleyl-2-lyso-phosphatidate	up
	2-R-hydroperoxy-linolenate	up
	(9Z)-12,13,17-trihydroxyoctadeca-9-enoate	up
	(9Z)-12,13-dihydroxyoctadeca-9-enoate	down
	dimorphecolate	down
	a 1-acyl-sn-glycero-3-phosphoglycerol (n-C14:1)	up
	1,3-dioctanoylglycerol	up
	10,16-dihydroxypalmitate	up
	18-oxo-oleate / 9,10-epoxy-12-cis-octadecenoate	down
	1-16:0-2-lysophosphatidylcholine	up
	1-18:2-2-16:3-monogalactosyldiacylglycerol	down
	1-18:3-2-16:2-monogalactosyldiacylglycerol	down
	1-18:3-2-16:3-monogalactosyldiacylglycerol	down
	1-18:3-2-trans-16:1-phosphatidylglycerol	up
Terpenes	a limonene-1,2-diol	up
	dehydroabietadiene-diol	down
	oryzalexin A	down
	3-beta-hydroxy-12,15-cassadiene-11-one	down
	9-beta-stemod-13(17)-en-19-oate	down
	kauralexin A2	up
	(6-E)-8-hydroxygeraniol	up
	heliocide B1/B2/B3/B4	up
	delta-tocotrienol	down
	oleanolate 3-beta-D-glucuronoside-28-glucoside	up
	medicagenate	up
	oleanolate 3-beta-D-glucuronoside	up
	glycyrrhetinate	up
	16-alpha-hydroxygypsogenate	up
	1,2-dihydrovomilenine	up
	13-desoxypaxilline	up
	3-hydroxyretinol	down
	prephytoene diphosphate	up
Gibberellins	gibberellin A15 (open lactone form)	up
	16-alpha- 17-epoxy gibberellin A12	up
	gibberellin A15 (closed lactone form)	up
	gibberellin A53	up
	gibberellin A110	up
	methyl gibberellin A20	up
	methyl gibberellin A4	up
	gibberellin A14	up
Jasmonates	(-)-jasmonoyl-L-isoleucine	up
	iso-jasmonoyl-L-isoleucine	up
Auxins	indole-3-acetyl-leucine / indole-3-acetyl-isoleucine	down
	indole-3-acetyl-phenylalanine	up
	alpha-naphthaleneacetamide	up
Cytokinins	isopentenyladenine-7/9-N-glucoside	up
Others	(+)-secoisolariciresinol diglucoside	up
	6-decylubiquinone	up
	N6-methyl-L-arginine	down
	8-methylthiooctylhydroximoyl-cysteinylglycine	up
	S-7-methylthioheptylhydroximoyl-L-cysteine	up
	4-(3-methylbut-2-enyl)-L-abrine	up
	homoarginine	down
	methoxydihydrosorgoleone	up
	9-mercaptodethiobiotin	up
	tylactone	up
	geissoschizine	up
	beta-fenchocamphorone	up
	1-phenyl-7-(3,4-dihydroxyphenyl)-hepta-1,3-dien-5-one	up
	(6S)-hydroxyhyoscyamine	up
	thebaine	up
	bestatin	up
	bornane-2,5-dione	down
	rhizobactin 1021 core	down
	cohumulone	up
	heptanal	up
	(iS/i)-nicotine	up
	chanoclavine-I	up
	aurachin C	up
	(+)-vernolate	down

secondary messengers, phytohormones regulating plant development (e.g., brassinosteroids), or defense substances (e.g., phytoecdysones) having a structure similar to that of the insect hormones. Our results demonstrated that all the discriminating steroids/sterols were more represented in the XS of S_{mng} plants at both ST1 and ST2 (Tables 1 and 2). Many of them are intermediates in the steroid biosynthetic patterns. Interestingly, ecdysone is an insect hormone with a steroid structure that controls the pupation of larvae. Plants can mimic these hormones, so that when insects eat plants containing phytoecdysones (triterpenoids), the pupation process is disturbed and the larvae die (Tarkowská and Strnad, 2016). It is hard to understand if the detected ecdysone was produced by insects (e.g., transmitted in the sap by aphid stylet or other insects) or if it was plant-synthesized. This compound was found to be more abundant in S_{mng} plants at ST1 (Table 1).

The physiological and phenological status of a plant is determined by its hormonal balance (Korovetska et al., 2016; De Ollas et al., 2018). The long-distance movement of many phytohormones from root to photosynthetic tissues through the xylem has been demonstrated (Lacombe and Achard, 2016), particularly for cytokinins (Yong et al., 2000; Lu et al., 2009), abscisic acid (Korovetska et al., 2016), but also for gibberellins, jasmonates, strigolactones and brassinosteroids. In particular, the biosynthetic patterns of many phytohormones are complex, intertwined and partly overlapping with those of many others primary and secondary metabolites (Heldt et al., 2005). The adoption of a S_{mng} caused an increase in some classes of phytohormones, and their conjugates and precursors, such as cytokinins (isopentenyladenine-7-*N*-glucoside and isopentenyladenine-9-*N*-glucoside), strigolactone precursors (tylactone at ST1 and carlactone at ST2), many gibberellins (especially at ST1), and jasmonates [(−)-jasmonoyl-L-isoleucine at both ST1 and ST2, and a jasmonoyl-1-aminocyclopropane-1 carboxylate at ST2) (Tables 1 and 2). All these phytohormones, excluding jasmonates that have mainly a defensive action, are secondary metabolites that in small amounts promote and regulate plant growth, development and differentiation of cells and tissues and, for this reason, they are also called “plant growth regulators” with PGP properties (Korovetska et al., 2016; De Ollas et al., 2018). A different case is that of auxins, whose transport is not mediated by xylem vessels (Lacombe and Achard, 2016). In our research, indole-3-acetic (auxin) precursors and degradation products were found in the xylem but never the final products (Tables 1 and 2). Interestingly, an auxin-like compound (α-

Table 2
Differential metabolites as provided by Volcano Plot analysis (*t*-test at $p < 0.01$ with Bonferroni multiple testing correction and fold-change > 5) in xylem sap metabolomic profile of olive plants grown under sustainable (S_{mng}) *vs* conventional (C_{mng}) soil at time point ST2 (October). Compounds are grouped in biochemical classes. The regulation (up or down) refers to the S_{mng} compared to C_{mng}.

Class	Compound	Regulation
Lipids	alpha-linolenate	up
	pinolenate	up
	gamma-linolenate	up
	2-omega-hydroxy-C22:0-LPA	up
	2-R-hydroperoxy-linolenate	up
	heptanoate	up
	(9Z)-12,13-dihydroxyoctadeca-9-enoate	up
	calendate	up
	alpha-eleostearate	up
	punicate	up
	dimorphecolate	up
	16-sinapoyloxypalmitate	up
	18-oxo-oleate	up
	1-18:0-2-18:3-phosphatidylethanolamine	up
	9,10-epoxy-12-cis-octadecenoate	up
	1-16:0-2-18:2-digalactosyldiacylglycerol	down
	1-18:2-2-16:0-digalactosyldiacylglycerol	down
	crepenynate	up
	ecdysone	up
	4-alpha-carboxy-4-beta,14-alpha-dimethyl-9-beta-19-cyclo-5-alpha-ergost-24-en-3-beta-ol	up
Terpenes	4,4'-diapolycopenedial	up
	levopiramadiene-diol	up
	dehydroabietadiene-diol	up
	neoabietadiene-diol	up
	dehydroabietadienol	up
	abieta-7,13-dien-18,18-diol	up
	palustradiene-diol	up
	isopimaradiene-diol	up
	neoabietadienal	up
	levopimaradienal	up
	palustradienal	up
	abieta-7,13-diene-18-al	up
	isopimaradienal	up
	9-beta-pimara-7,15-dien-19-al	up
	3-beta-hydroxy-12,15-cassadiene-11-one	up
	9-beta-stemod-13(17)-en-19-oate	up
	9-beta-stemod-13(17)-en-19-al	up
	ferruginol	up
	cyclooctatin	up
	kauralexin A1	up
	oryzalexin B	up
	oryzalexin D	up
	oryzalexin E	up
	oryzalexin F	up
	oryzalexin S	up
	oryzalexin A	up
	taxa-4,11-diene	up
	8-oxogeranial	down
	a 7-hydroxy-4-isopropenyl-7-methyloxepan-2-one	down
	geranylacetone	up
	heliocide B1	up
	heliocide B2	up
	heliocide B3	up
	heliocide B4	up
	oleanolate 3-beta-D-glucuronoside-28-glucoside	up
	glycyrrhetinate	up
	hederagenin	up
	alpha-curcumene	down
	heliespirone B	up
	abscisic alcohol	up
	germacra-1(10),4,11(13)-trien-12-al	up
	4-(5,5-dimethylcyclohex-1-en-1-yl)cyclohex-1-ene-1-carbaldehyde	up
Retinols	3-hydroxyretinol	up
	a retinol	up
Jasmonates	a jasmonoyl-1-aminocyclopropane-1 carboxylate	up
	jasmonoyl-L-isoleucine	up
	7-iso-jasmonoyl-L-isoleucine	up
Auxins	alpha-naphthaleneacetamide	down
	indole-3-butyryl-glucose	up
	10,11-epoxy-3-geranylgeranylindole	up
	13-desoxypaxilline	up
	indole-3-acetyl-phenylalanine	up
Phenolics	1-O-feruloyl-betaD-glucose	up
	1-phenyl-7-(3,4-dihydroxyphenyl)-hepta-1,3-dien-5-one	up
	coniferyl acetate	down
	taxa-4(20),11-dien-5-alpha,13-alpha-diol	up
	a rotenoid	up
	a 4'-methoxyisoflavone	up
Others	8-methylthiooctylhydroximoyl-cysteinylglycine	up
	S-7-methylthioheptylhydroximoyl-L-cysteine	up
	1,2-dihydrovomilenine	up
	geissoschizine	up
	carlactone	up
	1,7,9-tetramethylurate	up
	1,3,7,9-tetramethylurate	up
	2-methylpropanal-oxime	up
	Methyl-beta-D-glucoside 6-phosphate	up
	S-tetrahydroprotoberberine	up
	ent-kaurenal	up
	N-hydroxypentahomomethionine	up
	littorine	up
	N-caffeoylputrescine	up
	dethiobiotin	up
	3-geranyl-4-hydroxybenzoate	up
	piperazine-2-carboxamide	up
	7-methylthioheptanaldoxime	up
	13-hydroxylupanine	up
	hydroxyhyoscyamine	up
	thebaine	up
	N-isopropylformamide	up
	4-methyl-5-(beta-hydroxyethyl)thiazole	up
	1,2-di-S-octyl-1,2-dimercapto-3-propanol	up
	spinosyn tricyclic macrolactone	down
	11-dehydro-15-oxo spinosyn macrolactone	down
	bornane-2,5-dione	down
	rhizobactin 1021 core	up
	(S)-nicotine	up
	raucaffrinoline	up
	chanoclavine-I	up
	aurachin C	up
	juvenile hormone III	up
	dimeric urushiol peroxide	up
	(+)-vernolate	up

naphthaleneacetamide at ST1) and a degradation product of abscisic acid (*trans*-abscisic alcohol at ST2) were over-represented in the XS of S_{mng} plants (Tables 1 and 2). On the other side, jasmonates are partly xylem-borne hormones that have a PGP action (e.g., root elongation) and regulate stomata opening, but they also trigger both local and systemic defense responses (Lacombe and Achard, 2016; De Ollas et al., 2018).

Among the remaining compounds many free and conjugated phenols (1 at ST1 and 9 at ST2), lactones (3 at ST1 and 3 at ST1), purines (2 at ST2), oximes (3 at ST2), and other less represented compounds (lignans, carboxamides, alkanes/alkenes) were found at different concentrations between S_{mng} and C_{mng} plants. Among these compounds, phenols are likely the most important for plant defense and can be affected by different agronomic practices and environmental conditions, even if not always univocally (Sofo et al., 2016; Heimler et al., 2017). The S_{mng} provided soil with higher organic N and lower mineral N, and this likely was the reason of the increase in N-containing secondary metabolites (e.g., alkaloids and purines) and phenols, whose biosynthesis is generally induced when less nitrogen fertilizer is added to the soil (Heimler et al., 2017). Notably, flavonoids are also reported to modulate phytohormone signaling thus playing a functional role in plant-environment interactions (Brunetti et al., 2018).

Finally, other discriminating compounds between S_{mng} and C_{mng} plants included bacterial siderophores (rhizobactin 1021 core, produced by *Rhizobium* spp., at both ST1 and ST2), insect hormones and/or plant hormone-like compounds [(6 S)-hydroxyhyoscyamine at ST1, and ecdysone and juvenile hormone III at ST2], fungal fatty acids (crepenynate at ST2), natural insecticides produced by bacteria (spinosyn tricyclic macrolactone and 11-dehydro-15-oxo spinosyn macrolactone at ST2), intermediate products of camphor [e.g., β-fenchocamphorone at ST1 and (+)-bornane-2,5-dione at both ST1 and ST2], and biotin (9-mercaptodethiobiotin at ST1 and dethiobiotin at ST2).

3.3. Overview of the effects of soil management and sampling time on xylem sap composition

The majority of the discriminating compounds were found at significantly higher concentrations in the XS of S_{mng} plants, with the exception of some compounds of the following classes: retinols (ST1), indole-3-acetic acid conjugates (ST1), monoterpenoids (ST2) and spinosyn metabolites (ST2). From the overall data it emerges that the adoption of a S_{mng} for a long term determined a better plant status in terms of chemical defenses (e.g., terpenoids, alkaloids, phytoalexins, jasmonates, phenols), PGP phytohormones (e.g., gibberellins, cytokinins, strigolactones) and cell functionality (e.g., vitamin A, biotin, steroid second messengers). A S_{mng} including cover crops and internal C-inputs likely increased microbial diversity (Sofo et al., 2010, 2014; Pascazio et al., 2018), causing the presence of microbial-derived compounds beneficial for plants (siderophores, hormone-like substances, antibiotics).

Regarding the sampling time (ST1 and ST2), the 35 common compounds showed in the Venn diagram (Fig. 2) included mostly terpenoids (13), jasmonates (2), amino acids (2), alkaloid (3), being down-accumulated in the XS of S_{mng} plants. However, some steroids and retinols had an opposite trend at ST1 and ST2 (Tables 1 and 2). Interestingly, excepting for some auxin compounds (α-naphthaleneacetamide and 13-desoxypaxilline), hormones were not shared between the two sampling times (Tables 1 and 2). This suggests that the vegetative stage of olive plants played a pivotal role in determining the actual phytohormones profile in the XP, as already reported for auxins and abscisic acid by Sofo et al. (2018).

4. Conclusions

A sustainable orchard management is a key factor for enhancing soil fertility, *i.e.* the ability to supply the nutrients essential to plant growth (Sofo et al., 2010; Celano et al., 2011; Montanaro et al., 2012). Two additional key aspects are linked to soil fertility, namely: a) soil quality, *i.e.* the capacity of a soil to function within ecosystem boundaries to sustain biological productivity and promoting environmental, plant and animal health; and b) soil health, *i.e.* the continued capacity of a soil to function as a vital living ecosystem that sustains plants, animals, and humans. According to previous studies carried out in olive agro-ecosystems sustainably managed (Sofo et al., 2010, 2014; Pascazio et al., 2018), our data support that also xylem sap significantly responded to a shift of soil management toward a sustainable olive growing. The results of this study encourage the adoption of a set of sustainable agricultural practices (e.g., grass cover, pruning residues recycling, organic matter inputs) able to enhance plant physiological status, growth and natural defenses, with additional benefits on yield quantity/quality, the environment and human health.

Acknowledgments

The authors wish to thank the “Romeo ed Enrica Invernizzi” foundation for kindly supporting the metabolomics analytical platform. The authors thank Prof. Cristos Xiloyannis for the scientific support, Dr. Marina Scagliola for sap sample transportation and Prof. Carmine Crecchio for the revision of the manuscript. This work was supported by an OECD Co-operative Research Programme grant: Biological Resource Management tor Sustainable Agricultural Systems. Directorate: T AD/CRP; Contract: JA00091460.

Appendix A. Supplementary data

Supplementary data to this article can be found online at https://doi.org/10.1016/j.plaphy.2019.04.036.

Author contributions

AS, CF and AM designed and carried out the research. CF extracted the xylem sap from the trees. LL carried out the metabolomic analyses. LL and BD analyzed the data. AS and LL wrote the manuscript. All authors read and approved the manuscript.

Conflicts of interest

The authors declare that the research was conducted in the absence of any commercial or financial relationships that could be construed as a potential conflict of interest.

References

Alvarez, S., Marsh, E.L., Schroeder, S.G., Schachtman, D.P., 2008. Metabolomic and proteomic changes in the xylem sap of maize under drought. Plant Cell Environ. 31, 325–340. https://doi.org/10.1111/j.1365-3040.2007.01770.x.

Arisz, S.A., Testerink, C., Munnik, T., 2009. Plant PA signaling via diacylglycerol kinase. Biochim. Biophys. Acta - Mol. Cell Biol. Lipids 1791 869–875. https://doi.org/10.1016/j.bbalip.2009.04.006.

Brunetti, C., Fini, A., Sebastiani, F., Gori, A., Tattini, M., 2018. Modulation of phytohormone signaling: a primary function of flavonoids in plant–environment interactions. Front. Plant Sci. 9, 1–8. https://doi.org/10.3389/fpls.2018.01042.

Bruno, G., Sparapano, L., 2006. Effects of three esca-associated fungi on Vitis vinifera L.: II. Characterization of biomolecules in xylem sap and leaves of healthy and diseased vines. Physiol. Mol. Plant Pathol. 69, 195–208. https://doi.org/10.1016/j.pmpp.2007.04.007.

Carella, P., Wilson, D.C., Kempthorne, C.J., Cameron, R.K., 2016. Vascular sap proteomics: providing insight into long-distance signaling during stress. Front. Plant Sci. 7, 1–8. https://doi.org/10.3389/fpls.2016.00651.

Celano, G., Palese, A.M., Ciucci, A., Martorella, E., Vignozzi, N., Xiloyannis, C., 2011. Evaluation of soil water content in tilled and cover-cropped olive orchards by the geoelectrical technique. Geoderma 163, 163–170. https://doi.org/10.1016/j.geoderma.2011.03.012.

Dambrine, E., Martin, F., Carisey, N., Granier, A., H, J., Bishop, K., 1995. Xylem sap composition: a tool for investigating mineral uptake and cycling in adult spruce. Plant Soil 169–169, 233–241. https://doi.org/10.1007/BF00029333.

De Ollas, C., Arbona, V., Gómez-Cadenas, A., Dodd, I.C., 2018. Attenuated accumulation of jasmonates modifies stomatal responses to water deficit. J. Exp. Bot. 69, 2103–2116. https://doi.org/10.1093/jxb/ery045.

Dichio, B., Xiloyannis, C., Sofo, A., Montanaro, G., 2006. Osmotic regulation in leaves and roots of olive trees during a water deficit and rewatering. Tree Physiol. 26, 179–185. https://doi.org/10.1093/treephys/26.2.179.

FAO, 2006. Guidelines for Soil Description, fourth ed. Food and Agriculture Organization of the United Nations, Rome. http://www.fao.org/3/a-a0541e.pdf.

FAOSTAT, 2018. Accessed. http://faostat.fao.org, Accessed date: 12 October 2018.

Ferguson, A.R., Eisenman, J.A., Leonard, J.A., 1983. Xylem Sap from *Actinidia chinensis*: seasonal changes in composition. Ann. Bot. 51, 823–833. https://doi.org/10.1093/oxfordjournals.aob.a086533.

Heimler, D., Romani, A., Ieri, F., 2017. Plant polyphenol content, soil fertilization and agricultural management: a review. Eur. Food Res. Technol. 243, 1107–1115. https://doi.org/10.1007/s00217-016-2826-6.

Heldt, H.W., Piechulla, B., Heldt, F., 2005. Plant Biochemistry. Elsevier inc. https://doi.org/10.1046/j.1469-8137.1999.00517-1.x.

Korovetska, H., Novák, O., Turečková, V., Hájíčková, M., Gloser, V., 2016. Signalling mechanisms involved in the response of two varieties of *Humulus lupulus* L. to soil drying: II. changes in the concentration of abscisic acid catabolites and stress-induced phytohormones. Plant Growth Regul. 78, 13–20. https://doi.org/10.1007/s10725-015-0058-6.

Krishnan, H.B., Natarajan, S.S., Bennett, J.O., Sicher, R.C., 2011. Protein and metabolite composition of xylem sap from field-grown soybeans (*Glycine max*). Planta 233, 921–931. https://doi.org/10.1007/s00425-011-1352-9.

Lacombe, B., Achard, P., 2016. Long-distance transport of phytohormones through the plant vascular system. Curr. Opin. Plant Biol. 34, 1–8. https://doi.org/10.1016/j.pbi.2016.06.007.

Lima, M.R.M., Machado, A.F., Gubler, W.D., 2017. Metabolomic study of Chardonnay grapevines double stressed with esca-associated fungi and drought. Phytopathology

107, 669–680. https://doi.org/10.1094/PHYTO-11-16-0410-R.
Lu, Y.L., Xu, Y.C., Shen, Q.R., Dong, C.X., 2009. Effects of different nitrogen forms on the growth and cytokinin content in xylem sap of tomato (*Lycopersicon esculentum* Mill.) seedlings. Plant Soil 315, 67–77. https://doi.org/10.1007/s11104-008-9733-y.
Mazzafera, P., Gonçalves, K.V., 1998. Nitrogen compounds in the xylem sap of coffee. Phytochemistry 50, 383–386. https://doi.org/10.1016/S0031-9422(98)00582-2.
Meier, R., Ruttkies, C., Treutler, H., Neumann, S., 10 November 2017. Bioinformatics can boost metabolomics research. J. Biotechnol. 261, 137–141. https://doi.org/10.1016/j.jbiotec.2017.05.018.
Montanaro, G., Dichio, B., Briccoli Bati, C., Xiloyannis, C., 2012. Soil management affects carbon dynamics and yield in a Mediterranean peach orchard. Agric. Ecosyst. Environ. 161, 46–54. https://doi.org/10.1016/j.agee.2012.07.020.
Palese, A.M., Vignozzi, N., Celano, G., Agnelli, A.E., Pagliai, M., Xiloyannis, C., 2014. Influence of soil management on soil physical characteristics and water storage in a mature rainfed olive orchard. Soil Tillage Res. 144, 96–109. https://doi.org/10.1016/j.still.2014.07.010.
Pascazio, S., Crecchio, C., Ricciuti, P., Palese, A.M., Xiloyannis, C., Sofo, A., 2015. Phyllosphere and carposphere bacterial communities in olive plants subjected to different cultural practices. Int. J. Plant Biol. 6. https://doi.org/10.4081/pb.2015.6011.
Pascazio, S., Crecchio, C., Scagliola, M., Mininni, A.N., Dichio, B., Xiloyannis, C., Sofo, A., 2018. Microbial-based soil quality indicators in irrigated and rainfed soil portions of Mediterranean olive and peach orchards under sustainable management. Agric. Water Manag. 195. https://doi.org/10.1016/j.agwat.2017.10.014.
Rouphael, Y., Colla, G., Bernardo, L., Kane, D., Trevisan, M., Lucini, L., 2016. Zinc excess triggered polyamines accumulation in lettuce root metabolome, as compared to osmotic stress under high salinity. Front. Plant Sci. 7, 842. https://doi.org/10.3389/fpls.2016.00842.
Salehi, H., Chehregani, A., Lucini, L., Majd, A., Gholami, M., 2018. Morphological, proteomic and metabolomic insight into the effect of cerium dioxide nanoparticles to *Phaseolus vulgaris* L. under soil or foliar application. Sci. Total Environ. 616–617, 1540–1551. https://doi.org/10.1016/j.scitotenv.2017.10.159.
Sofo, A., Benjeddou, H., Fourati, R., Ahmed, C., Ben, Rouina, B., Ben, Galgano, F., Caruso, M.C., Casacchia, T., Scopa, A., 2018. Characterization of biochemical factors affecting crop load in three olive cultivars. Eur. J. Hortic. Sci. 83, 28–34. https://doi.org/10.17660/eJHS.2018/83.1.4.
Singh, B., Sharma, R.A., 2015. Plant terpenes: defense responses, phylogenetic analysis, regulation and clinical applications. 3 Biotech 5, 129–151. https://doi.org/10.1007/s13205-014-0220-2.
Sofo, A., Ciarfaglia, A., Scopa, A., Camele, I., Curci, M., Crecchio, C., Xiloyannis, C., Palese, A.M., 2014. Soil Microbial Diversity and Activity in a Mediterranean Olive Orchard Using Sustainable Agricultural Practices. Soil Use Manag. https://doi.org/10.1111/sum.12097.
Sofo, A., Lundegårdh, B., Mårtensson, A., Manfra, M., Pepe, G., Sommella, E., De Nisco, M., Tenore, G.C., Campiglia, P., Scopa, A., 2016. Different agronomic and fertilization systems affect polyphenolic profile, antioxidant capacity and mineral composition of lettuce. Sci. Hortic. (Amst.) 204, 106–115. https://doi.org/10.1016/j.scienta.2016.04.003.
Sofo, A., Palese, A.M., Casacchia, T., Celano, G., Ricciuti, P., Curci, M., Crecchio, C., Xiloyannis, C., 2010. Genetic, functional, and metabolic responses of soil microbiota in a sustainable olive orchard. Soil Sci. 175. https://doi.org/10.1097/SS.0b013e3181ce8a27.
Sorce, C., Massai, R., Picciarelli, P., Lorenzi, R., 2002. Hormonal relationships in xylem sap of grafted and ungrafted Prunus rootstocks. Sci. Hortic. (Amst.) 93, 333–342. https://doi.org/10.1016/S0304-4238(01)00338-7.
Tarkowská, D., Strnad, M., 2016. Plant ecdysteroids: plant sterols with intriguing distributions, biological effects and relations to plant hormones. Planta 244, 545–555. https://doi.org/10.1007/s00425-016-2561-z.
Tsugawa, H., 2018. Advances in computational metabolomics and databases deepen the understanding of metabolisms. Curr. Opin. Biotechnol. 54, 10–17. https://doi.org/10.1016/j.copbio.2018.01.008.
Yong, J.W., Wong, S.C., Letham, D.S., Hocart, C.H., Farquhar, G.D., 2000. Effects of elevated [CO_2] and nitrogen nutrition on cytokinins in the xylem sap and leaves of cotton. Plant Physiol. 124, 767–780. https://doi.org/10.1104/pp.124.2.767.

Table S1. Whole dataset on xylem sap metabolomic profile of olive plants grown either under sustainable (Smng) and conventional (Cmng) soil management and at two different time points (ST1: May; ST2: October). Individual abundances are provided together with composite spectrum (mass and abundance combinations) of each compound annotated.

Compound
7-oxatyphasterol
1-18:3-16:0-monogalactosyldiacylglycerol
citronellate
(12Z,15Z)-9,10-epoxyoctadeca-12,15-dienoate
cinchonine
cinnamoyltyramine
parthenolide
(S)-sinapoylcholine
(R)-mandelonitrile
cyclooctat-9-en-7-ol
N-acetyl-D-galactosamine
N/sup1/sup-acetylspermine
marmesol
pentalenolactone D
a carvone
2-heptyl-4(1H)-quinolone
6-oxocampestanol
(6α)-hydroxycampestanol
18'-hydroxy-χ,χ-caroten-18-oate
2-pentadecanone
lithocholate
χ,χ-caroten-18-oate
cathasterone
(-)-ephedrine
7-dehydrodesmosterol
4α-hydroxymethyl-4β,14α-dimethyl-9β,19-cyclo-5α-ergost-24(24sup1/sup)-en-3β-ol
thalianol
(S)-nicotine
2-ω-hydroxy-C22:0-LPA
N-carbamoylputrescine
4-prenylphlorisovalerophenone
(3S)-2,3-epoxy-2,3-dihydrosqualene
oleanolate 3-β-D-glucuronoside-28-glucoside
feruloylagmatine
4α,14α-dimethyl-ergosta-8,25(27)-dienol
5α-cholesta-8,24-dien-3-one
4α,14α-dimethyl-5α-cholesta-8,24-dien-3β-ol
Ψ-taraxasterol
2-fluorobenzoate
ergosta-7,25(27)-dienol
prostaglandin Dsub2/sub
leukotriene Bsub4/sub
(6E)-8-hydroxygeraniol
cycloartenol
D-ornithine
8-methylthiooctylhydroximoyl-cysteinylglycine
1-18:3-trans-16:1-phosphatidylglycerol
anandamide
monofluoromethylputrescine
(E,E)-farnesylacetone
erythrodiol
(20R),22R-dihydroxycholesterol
5-fluorocytosine
pentahomomethionine
17β-estradiol
(9S,10S)-9,10-dihydroxyoctadecanoate
(22α)-hydroxy-campest-4-en-3-one
secalciferol
5-dehydroavenasterol
myconamicin III
pregnenolone
16,17-dihydro-16α,17-dihydroxy gibberellin Asub4/sub
gibberellin Asub15/sub (open lactone form)
3-dimethylsulfoniopropionaldehyde
L-dihydrophenylalanine
colneleate
α-linolenate
typhasterol
diploxigenin 3-O-β-D-quinovoside
16β-hydroxy-β-amyrin
spurulenol
eudesmol, bisabolol, etc
montanate
scalar-17(25)-en-19-ol
calendate
(3S,5R,6R)-3,5-dihydroxy-6,7-didehydro-5,6-dihydro-12'-apo-β-caroten-12'-al
(E,E)-geranyllinalool
(-)-helianuol E
2-C22:0-DCA-LPA
1-monopalmitoylethylene glycol
a retinal
17-β-hydroxyandrostan-3-one
crepenynate
porifersta-8,25(27)-dienol
(-)-9β-pimara-7,15-dien-19-al
1,2-dihydrovomilenine
all-trans-4,4'-diaponeurosporene
30-hydroxy-β-amyrin
NSUP4/SUP-acetyl-NSUP4/SUP-hydroxy-1-aminopropane
a methyl jasmonate
3-methoxytyramine
campest-4-en-3β-ol
dihydroferulate
1-18:1-2-18:1-phosphatidate
1-pyrroline-4-hydroxy-2-carboxylate
2-hydroxy-1,4-benzoquinone
γ-solanine
methyl gibberellin Asub9/sub
texasterone
ent-2α-hydroxykaurene
D-glutamine
14-oxolanosterol
18-oxo-oleate
ω-hydroxylaurate
cyclooctat-9-en-5,7-diol
Δsup9/sup-tetrahydrocannabinolate
2,3-bis-O-phytanyl-sn-glycerol 1-phosphate
(S)-2-hydroxyglutarate
oleate
methyl-1,4-benzoquinol
a vaccenate
4α,14α-dimethyl-9β,19-cyclo-5α-cholest-24-en-3-one
a 4-hydroxysphing-8-enine-22:0 ceramide
3β-hydroxy-12,15-cassadiene-11-one
aclacinomycin T
urushiol III
9β-stemod-13(17)-en-19-oate
a C34 botryococcene
18-hydroxyoleate
2-nitrobenzoate
(13E)-labda-7,13-dien-15-ol
manoyl oxide
6-deoxocathasterone
(2Z,4E)-2-hydroxy-6-oxohexa-2,4-dienoate
protopanaxatriol
8-aminooctan-4-one
erythro-4-hydroxy-L-glutamate
diprenylphlorisovalerophenone
3β-hydroxy-4β-methyl-5α-cholest-7-ene-4α-carbaldehyde
alendronate
geranylgeraniol
N-methyl-DL-aspartate
FK-506
2-hydroxyhexadecanoate
α,ω-9Z-octadecenedioate
methoxydihydrosorgoleone
neoabietadienol
(1R,5R)-sabinene
4α-formyl-4β,14α-dimethyl-9β,19-cyclo-5α-cholest-24-en-3β-ol
dimethylsulfonio-2-hydroxybutanoate
5-α-dihydrotestosterone
2-hydroxyglutarate
N-acetyl-β-neuraminate
(S)-allyl-L-cysteine
an N-acetyl-β-D-hexosamine
4,8-sphingadienine
ornithine
8-amino-7-oxononanoate
3-oxo-myristate
(9Z,12Z)-octadecadien-6-ynoate
caloxanthin
levopimaradienal
an 11,13-eicosadienoate
8-methylthiooctanonitrile oxide
decanoate
N-acetyl-β-glucosaminylamine
22-oxo-docosanoate
medicagenate
all-trans-3-hydroxyretinal
4α-carboxy-ergosta-7,24(24sup1/sup)-dien-3β-ol
15-cis-phytoene
9,10-epoxy-18-hydroxystearate
a glutamate
9β-stemod-13(17)-en-19-al
4α-hydroxymethyl-4β-methyl-5α-cholesta-7,24-dien-3β-ol
5α-cholesta-8-en-3-one
(24R)-24-methylcycloarta-25-en-3β-ol
16α,17-epoxy gibberellin Asub12/sub
N-acetyl-β-D-glucosaminyl-(1→4)-D-glucosamine
pinolenate
homofuraneol
(S)-(2E,6E)-farnesyl-L-cysteine
4α-methyl-5α-cholesta-8,14,24-trien-3β-ol
desacetoxyvindoline
cycloeucalenol
4α-methyl-zymosterol
aphidicolan-16β-ol
24-epicathasterone
adhyperforin
labd-13-en-8β,15-diol
stevioside
4-coumaroylagmatine
10,11-epoxy-3-geranylgeranylindole
stearidonate
episterone
α-fenchocamphorone
prephytoene diphosphate
L-threo-sphinganine
30-hydroxy-11-oxo-β-amyrin
(S)-[2-(4-hydroxyphenyl)acetaldehyde oxime]
3-dehydro-4-methylzymosterol
taraxasterol
a 4-hydroxysphing-8-enine-20:1 ceramide
4α-hydroxymethyl-stigmasta-7,24(24sup1/sup)-dien-3β-ol
tricoumaroyl spermidine
2,7-dihydroxycadalene
ajmaline
(R,S)-piperazine-2-tert-butylcarboxamide
phylloquinone
N-acetyl-β-D-glucosamine
gibberellin Asub15/sub (closed lactone form)
4α-formyl-5α-cholesta-7,24-dien-3β-ol
1,2-dioctanoyl-1,2,6-hexanetriol
26-hydroxybrassinolide
α-eleostearate
β-seco-amyrin
perillate
δ-tocotrienol
melamine
3-ureidopropionate
benzylglucosinolate
5-1-(4-hydroxyphenyl)-ethanol
β-phellandrene
17-O-acetylajmaline
palmitaldehyde
16-hydroxytabersonine
momilactone A
ent-7α-hydroxykaur-16-en-19-oate
cinchonine
momilactone B
4α-methyl-5α-cholesta-8-en-3-one
24-hydroxy-β-amyrin
obtusifoliol
melissate
poriferst-7-enol
adonixanthin
(5Z)-(15S)-11-α-hydroxy-9,15-dioxoprosta-13-enoate
5α-cholesta-7,24-dien-3-one
4-fluorobenzoate
(9R,10S)-dihydroxystearate
9-mercaptodethiobiotin
a rotenoid
(4S)-limonene
docosanedioate
prostaglandin Esub2/sub
zymosterol
2-tridecanone
5α-cholestan-3-one
(5α)-campestan-3-one
3,20-dimethyl-1,2,21,22-tetradehydro-2,3,20,21-tetrahydrobotryococcene
demethylphylloquinone
4α-hydroxymethyl-4β-methyl-5α-cholest-7-en-3β-ol
L-glutamate
(22R,23R)-28-homocastasterone 22-O-sulfate
capsaicin
14-hydroxylanosterol
5-[(4-methoxy-3-(phenylmethoxy)phenyl)methyl]-2,4-pyrimidinediamine
methyl 7-(R)-glucose
methylionone
sterculate
dammarenediol II
(9Z,12Z)-15,16-epoxyoctadeca-9,12-dienoate
levopimaradienol
9,10,18-trihydroxystearate
8-hydroxyprenyl-linolenate
α-tocotrienol
D-alanyl-D-lactate
(E)-β-ocimene
1,2-dipalmitoylglycerol
ent-sandaracopimaradiene-3β-ol
2α-hydroxy-ent-cassadiene
β-myrcene
(-)-β-pinene
4α-methyl-5α-ergosta-8,14,24(28)-trien-3β-ol
1-16:0-2-lysophosphatidylcholine
campest-4-en-3-one
dATP
11-cis-3-hydroxyretinal
campesterol
a 4'-methoxyisoflavone
2-decenol
all-trans-3-hydroxyretinol
oleanolic aldehyde
3-ureido-isobutyrate
thymine
2-methyl-6-farnesyl-1,4-benzoquinol
dihydrozeatin-9-N-glucoside
7,8-dihydropterin
ferruginol
(+)-camphene
cholesterol
3-hydroxy-16-methoxy-2,3-dihydrotabersonine
4-hydroxy-5-methyl-2-methylene-3(2H)-furanone
L-methionine-S-oxide
bixin aldehyde
4α-methyl-5α-cholest-7-en-3-one
palustradienol
oryzalide A
BPH-698
brassinolide-23-O-glucoside
ubiquinone-2
vernoleate
1-18:3-2-16:4-monogalactosyldiacylglycerol
glycyrrhetaldehyde
4-hydroxy-trans-8-sphingenine
2,3-bis[(3R)-3-hydroxymyristoyl]-α-D-glucosaminyl 1-phosphate
tylactone
α-3',4'-anhydrovinblastine
a limonene-1,2-diol
gypsogenate-28-beta-D-glucoside
camelliol C
(R)-(-)-carvone
4-prenylphlorisobutyrophenone
2,2,6,9-tetramethyl-5,6-dihydro-2H-1-benzooxocine-3,8-diol
leukotriene Asub4/sub
24-methylenelophenol
1-18:1-2-18:1-sn-glycerol-3-phosphocholine
phenylacetyl-CoA
3-(6'-methylthio)hexylmalate
4α-methyl-5α-cholesta-7,24-dien-3β-ol
12,13β-epoxy-β-amyrin
31-O-demethylFK-506
gibberellin Asub53/sub
2-heptyl-3-hydroxy-4(1H)-quinolone
β-terpinene
(3S,5R,6S)-5,6-epoxy-3-hydroxy-5,6-dihydro-12'-apo-β-caroten-12'-al
5'-hydroxy-rot-2'-enonate
renierapurpurin
(22R,23R)-22,23-dihydroxy-campest-4-en-3-one
rebaudioside B
muconolactone
isoserbonol
16-sinapoyloxypalmitate
ent-16α-hydroxy-kaurene
26-hydroxycastasterone
6-deoxo-24-epicathasterone
3-methoxy-5-hydroxytoluene
7-oxateasterone
a 4-hydroxy-8-sphingenine
geissoschizine
nicotinamide
a jasmonoyl-1-aminocyclopropane-1-carboxylate
4,8,12-trimethyl-1,3,7,11-tridecatetraene
isofucosterol
strombine
indolin-2-one
all-trans-13,14-dihydroretinol
squalene
2-methylaspartate
a 1-octadec-11-enoyl-sn-glycerol 3-phosphate
3-propylphosphoenolpyruvate
emindole-SB
vernolate
solasodine 3-O-β-D-glucopyranoside
parkeol
4-tyrosol
crocetin dialdehyde
fusidate
all-trans-10'-apo-β-carotenal
sphingosine
lathosterol
taxa-4(20),11-dien-5α,13α-diol
6-deoxocastasterone
methanophenazine
(+)-vernolate
2-acetamido-4-O-(2-amino-2-deoxy-β-D-glucopyranosyl)-2-deoxy-D-glucose
baruol
5-isobutylthiophene
5α-cholesta-7,24-dien-3β-ol
(9Z,15Z)-12,13-epoxy-octadeca-9,15-dienoate
(R)-mandelate
2,3-bis-O-(geranylgeranyl)glycerol 1-phosphate
solanidine
taraxerol
bixin dimethyl ester
4-amino-2-methyl-5-diphosphomethylpyrimidine
3-methylxanthine
sphinganine
antheraxanthin
pyridoxamine
9β-stemod-13(17)-en-19-ol
arachidonate
hyperforin
2-cis-abscisate
tetrahomomethionine
(22α)-hydroxy-campesterol
4α-hydroxymethyl-ergosta-7,24(24sup1/sup)-dien-3β-ol
N-acetyl-D-glucosamine
24-methylenecycloartanol
terpineolo, linalool, menthone, citronellale
conferonate
(S)-norlaudanine
24-epi-campesterol
N3-methylcytosine
gibberellin Asub110/sub
betulinic aldehyde
γ-linolenate
ergosta-5,7-dienol
5-α-pregnane-3,20-dione
quinine
3-carene
all-trans-geranyl-geranyl monophosphate
14,15-epoxyemindole-SB
ergosterol
humulone
3-hydroxyechinenone
an α-pinene
bauerenol
N(SUP1/SUP)-acetylspermidine
paspaline
4α-hydroxymethyl-4β,14α-dimethyl-9β,19-cyclo-5α-cholest-24-en-3β-ol
11-cis-3-hydroxyretinol
5-oxoproline
8-amino-2,6-anhydro-3,8-dideoxy-D-glycero-D-talo-octonate
pseudoephedrine
(2-aminoethyl)phosphonate
(5Z)-(15S)-11α-hydroxy-9,15-dioxoprostanoate
pseudotropine
(R)-reticuline
24-epicathasterone-22-O-sulfate
an N-acetyl-D-hexosamine
terpinolene
estrone
7,8-diaminopelargonate
alanopine
octan-1-ol
(9Z)-(13S)-12,13-epoxyoctadeca-9,11-dienoate
2,3-dioctanoylglyceramide
aklanonate
6β-hydroxy-syn-pimaradiene
raucaffrinoline
dehydroabietadiene-diol
9-methylthiononanonitrile oxide
D-xylonolactone
(3R,7S)-12-hydroxy-jasmonoyl-L-isoleucine
5-pentadecatrienyl resorcinol-3-methyl ether
4α-formyl-5α-cholesta-8,24-dien-3β-ol
ricinoleate
D-fructosyl-L-lysine
N-acetyl-D-mannosamine
cholesteryl-β-D-glucoside
conhydrine